V European Conference on Computational Fluid Dynamics
ECCOMAS CFD 2010
J. C. F. Pereira and A. Sequeira (Eds)
Lisbon, Portugal, 14–17 June 2010

# SPH SIMULATIONS OF FREE SURFACE WAVES AND THE INTERACTION WITH OBJECTS

**Paul H.L. Groenenboom[*], Bruce K. Cartwright[†]**

[*] ESI Group Netherlands
Rotterdamseweg 183 C, 2629 HD Delft, The Netherlands
e-mail: Paul.Groenenboom@esi-group.com

[†] Pacific Engineering Systems International Pty Ltd
277-279 Broadway, Broadway NSW 2007, Australia
e-mail: brucec@esi.com.au

**Key words:** Smoothed Particle Hydrodynamics, Finite Elements, Fluid-structure interaction, Free Surface Waves, Ditching

**Abstract.** *This paper discusses the Smoothed Particle Hydrodynamics (SPH) method as an integral part of the explicit finite element (FE) program PAM-CRASH and its application to free surface waves. Some of the application areas include the interaction of waves with floating objects and the water entry of dropped objects into both quiescent and wavy sea states. The Lagrangian nature of the SPH method facilitates the modeling of large changes in the geometry and even topology both of the free surface and of the structural interface. This makes the method suitable for the simulation of ships and other floating structures in water even in the presence of breaking waves. A numerical technique that creates regular waves with a low amount of dispersion or other numerical losses has been developed and validated [1, 2]. Its combination with periodic boundary conditions will be shown, using several case studies, to yield a powerful method for the generation of regular waves during a sufficiently long period of time to study the response of a vessel subjected to such waves. Armed with such a numerical tool to model fluid-structure interactions [2], one can investigate slamming, sloshing and water entry. The application to objects ranging from very simple geometry through to complex engineering structures such as free fall lifeboats, ditching helicopters with flotation devices and a disabled submarine, will be discussed.*

## 1 INTRODUCTION

There are many physical scenarios where the combination of free surface waves and fluid-structure interaction has to be considered and for which numerical simulation provides greater engineering insight. However, the effective simulation of free surface waves is a challenge for most numerical methods, especially when the wave amplitude may no longer be considered small compared to the wave length. This is often the case when potentially damaging waves hit ships or other floating structures and especially true when slamming occurs. The numerical challenges become nearly insurmountable when structural deformations have to be considered.

Herein the authors discuss the Smoothed Particle Hydrodynamics (SPH) method that can simulate dynamic flow including large changes both in the free surface geometry and in the deformable interface. The SPH method used herein is implemented within the PAM-CRASH [3] general purpose, finite-element (FE) based, commercial structural dynamics code. Sections 2 and 3 respectively look into the numerical methodology and the specifics of the generation of waves. The impact of a flexible cylinder onto water used to validate the method is discussed in section 4, while the remaining sections deal with practical engineering applications such as the response of a frigate in high seas, the ditching of a helicopter and the behavior of a disabled submarine in the ocean.

## 2 NUMERICAL METHODS EMPLOYED

### 2.1 Overview

The SPH method is an interpolation method in which each "particle" describes a fixed amount of material in a Lagrangian reference frame. Despite its appearance as a collection of points, SPH is aimed at solving continuum mechanics of fluids and solid materials. Since the method does not require a mesh, SPH handles the motion and topology changes of material surfaces quite simply. The evaluation of the relevant field variables such as density and velocity at the location of a selected particle is conducted by interpolation over all neighbor particles in a region of influence as illustrated in Figure 1. The size of the sphere (or circle in 2D) of this region, is defined by a smoothing length, *h*. A key advantage of the SPH method is that spatial derivatives of the unknown field variables may be evaluated using the known derivative of the smoothing kernel.

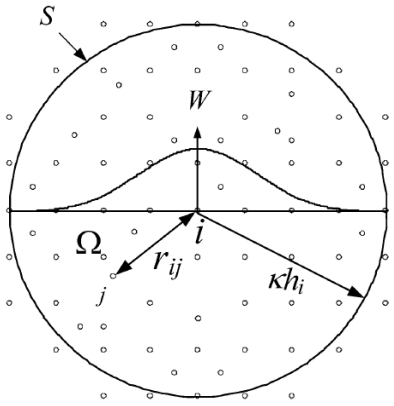


Figure 1: Two-dimensional representation of the region of influence of particle 'i'

Unless mentioned otherwise, the SPH method discussed here is basically similar to that of Monaghan [4, 5]. Within the SPH method, the derivative of the density for particle *i* may be solved from the continuity equation 1:

$$\frac{D\rho}{Dt} = \sum_{j=1}^{N} m_j v_{ij}^{\beta} \frac{\partial W_{ij}}{\partial x_i^{\beta}} \tag{1}$$

where the sum extends over all neighbor particles and W is the smoothing kernel evaluated at the distance between particles *i* and *j*. Optionally, renormalization of the density field may be performed.

The updated velocity may be obtained from the momentum equation 2:

$$\frac{Dv^{\alpha}}{Dt} = \sum_{j=1}^{N} m_j \left( \frac{\sigma_i^{\alpha\beta}}{\rho_i^2} + \frac{\sigma_j^2}{\rho_j^2} \right) \frac{\partial W_{ij}}{\partial x_i^{\beta}} + F_i \tag{2}$$

Additionally, the artificial viscosity needs to be included as:

$$\Pi_{ij} = \begin{cases} \dfrac{-\alpha_{\Pi}\overline{c_{ij}}\phi_{ij} + \beta_{\Pi}\phi_{ij}^2}{\overline{\rho_{ij}}} , & v_{ij}x_{ij} < 0 \\ = 0 , & v_{ij}x_{ij} \geq 0 \end{cases} \tag{3}$$

where,

$$\phi_{ij} = \frac{h_{ij} v_{ij} . x_{ij}}{|x_{ij}|^2 + \varphi^2}$$

$$\bar{c}_{ij} = \frac{1}{2}(c_i + c_j)$$

$$\bar{\rho}_{ij} = \frac{1}{2}(\rho_i + \rho_j)$$

$$h_{ij} = \frac{1}{2}(h_i + h_j)$$

$$v_{ij} = v_i - v_j , \; x_{ij} = x_i - x_j$$

The values α and β determine the strength of the artificial viscosity required to suppress numerical shocks. If there are no shocks present, these parameters should be set to low values to prevent the flow becoming too viscous. Regular particle positions are achieved when the particle motion correction or anti-crossing option (XSPH) [4] is employed, as expressed in Equation 4.

$$\frac{d\mathbf{r}_i}{dt} = v_i + \varepsilon \sum_j m_j \frac{v_{ij}}{\rho_{ij}} W_{ij} \tag{4}$$

For a non-zero ε parameter, equation 4 is used to update the particle positions, whereas the strains remain based on the uncorrected displacements. The cubic spline kernel is used for the smoothing kernel, where the smoothing length, h, is proportional to the particle radius.

The flow will be assumed to be nearly incompressible implying that the pressure field is obtained from an equation of state (EOS) model. For water, either a polynomial EOS, or the Murnaghan model as shown in Equation 5, is used.

$$p = p_0 + B\left(\left(\frac{\rho}{\rho_0}\right)^{\gamma} - 1\right) \tag{5}$$

A cut-off pressure may be included as a simple approximation to cavitation.

Particles are assumed to interact mutually only if they are sufficiently close to each other; this being established by a nearest neighbor (NN) search algorithm that, for efficiency reasons, does not need to be repeated at each computational cycle. Second-order accurate leap-frog time stepping is used for the explicit time integration of the above rate equations. The numerical time step is set at a fraction, usually about 0.7, of the well-known CFL criterion based on the current size of, and sound speed within, all the particles and finite elements present in the model.

### 2.2 Coupling with Finite Elements for fluid-structure interaction

The general purpose FE code used is build around an explicit solver optimized for the analysis of highly non-linear structural dynamical behaviour, and contains element formulations for thin shells, solid elements, membranes and beams with material models for plasticity and failure for metals, plastics, rubbers, foams and composites. The code contains robust contact, including sliding interface, algorithms to model the dynamic contact between various parts within a model. The solver allows both finite elements and (the SPH method's) particles to be used simultaneously within the same model, with optimal performance achieved by using either the Distributed Memory Parallel (DMP) or the Shared Memory Parallel (SMP) version.

Interaction between particles representing a fluid and moving or deformable structures may be modelled by one of the contact algorithms just mentioned. Such algorithms, while allowing sliding at the interface, prevent penetration between selected structures. Their implementations are based on the well known penalty formulation, where geometrical interpenetrations between so-called slave nodes and adjacent master faces are penalized by counteracting forces that are essentially proportional to the penetration depth. The contact algorithm will automatically detect when a particle (slave) penetrates any segments (master) of the outer surface of the finite element model of the structure. The contact thickness indicates the distance away from a contact face where physical contact is established. For SPH particles as slaves, the contact thickness should be representative of the particle spacing. This type of contact has been validated by the vertical motion of floating bodies. It has been found that the correct position is reached when the thickness defined for the contact is half the particle spacing and the artificial viscosity coefficients are significantly smaller than the values normally applied for shocks. In that case the upward force is also correct. The use of coupled SPH-FE has

been used for many applications such as sloshing [6], the opening of a heart valve [7], the impact of birds onto aeronautical structures [8], or lifeboat drop [9] onto water.

In addition, it is possible to define a tied contact in which virtual spring elements are automatically defined between particles that are sufficiently close to segments in the initial configuration. Such a contact acts as a rigid connection between the two parts.

### 2.3 Hydrostatic pressure initialisation

For many hydrodynamic simulations involving a free surface, a significant amount of computer time may be expended to reach hydrostatic equilibrium under gravity in the water before the event of interest can start. An option has been implemented that allows initializing the hydrostatic pressure at the start of the simulation. This may be done for an assembly of particles representing a single density liquid in which case the position of the free surface is evaluated automatically, or for finite volume elements in which the free surface location has to be provided by the user. For each particle, or the centre of gravity of each solid element, the distance to the free surface in the direction of the gravity as specified by the user is evaluated and the initial density is multiplied by an exponential function of this distance. It must be assumed that the reference density is the same along the line in this direction and that there exists a unique location of the free surface. Although the hydrostatic pressure is likely to change when the water is settling into a container acting as a boundary for a finite volume of water, these changes are small with respect to the changes required without this option. Hence, computer time may be reduced when this option is exploited.

### 2.4 Gauges for pressure and free surface level

For hydrodynamic simulations with SPH, it is convenient to define the concept of gauge nodes. These gauges may be defined as moving along with the structure (as FE nodes), given a fixed motion (as free nodes), or as particles. Their use enables information about the pressure to be obtained at any desired location. Note that since the pressure will be averaged over a number of nearby particles, it will not suffer from the strong spatial fluctuations typical for the pressure for individual particles. For many hydrodynamics applications it is interesting, and even critical, to know the current free surface location. Gauges are defined as a special type of particles for which no force calculation is made and which also do not contribute to the evaluation of SPH properties of regular particles. This is accomplished by the definition of a flag for the particles. The pressure at the gauges is located by taking the average using the smoothing kernel over the current neighbouring particles within a smoothing length defined by the user. Tests have indicated both that the pressures evaluated by gauge points have the same smoothed appearance as the particle pressures and that they correspond to the hydrostatic values in the case of equilibrium. The free surface level is evaluated by an iterative procedure that searches for the coordinate in a given direction where the SPH particle density equals one half. This definition is the most appropriate one to determine the location of singly-defined free surface for a given direction, although in the case of over-turning waves or splashing, this definition may not be unique.

### 2.5 Periodic boundary conditions

For studies involving undisturbed flow or free-surface wave propagation in extended domains, the option of periodic boundary conditions significantly reduces the number of particles required. For SPH, a rectangular box is defined where, as soon as a particle

crosses a boundary face, it is injected at the opposite face with the same velocity and material properties. When due care is taken such that the neighbour search of all particles extends over the faces of the domain, the flow remains undisturbed.

## 3 WAVE GENERATION FOR SPH

A novel method of wave generation is employed that develops a free-surface wave in a fluid domain of arbitrary size and shape. The authors have previously demonstrated that with the SPH method, it is possible to generate first-order waves that may be used for ship motion in both severe conditions [10] and more benign sea states [11]. The waves used in this paper will be considered to be deep water waves for which the water motion at a depth beyond the limit of about half a wavelength has become small enough to be neglected. Second-order Stokes' waves will be assumed.

To reduce computer resources, the domain depth will be chosen to be less than this limit. In that case, the domain floor can no longer be assumed to remain at rest but will be assigned the displacement field corresponding to the analytical approximation for the undisturbed waves. Another reason to assign the undisturbed wave motion to the floor is to counteract any losses in the wave amplitude usually observed when a wave series traverses an extended domain of sufficient depth but can still be represented by a computationally acceptable number of particles. Similar displacement conditions will be assigned to all other walls enclosing the domain. In case the waves are disturbed by floating or dropped objects, the location of the boundaries needs to be chosen sufficiently far away from the objects that the reflection of any wave disturbance can safely be ignored. For obvious reasons of consistency, the boundaries are defined in the same Lagrangian reference frame as the particles.

The wave field within the domain is developed by gradually increasing the domain boundary displacements from zero to the fully developed displacement amplitudes as governed by the specific boundary node location in an otherwise fully developed wave field of infinite domain. The particles within the domain boundaries subsequently acquire displacements through the SPH interaction laws. The time to fully develop the wave field by this technique is typically less than two periods.

An interesting feature of this mode of wave generation occurs when the domain length is many wavelengths long. In this case the time to fully develop the wave field throughout the domain is less than the time taken for the slowest wave to traverse the domain. In addition, and relevant to a domain of any size, the time to develop the wave field may be eliminated entirely if each SPH element within the domain was assigned an initial displacement and velocity that coincided with the fully developed wave field. In this case the ramp-up period is not required, reducing the CPU time. This feature has been demonstrated in a development version of the commercial code.

In a test case for second-order deep water waves in a two-dimensional section, the wave length was set to 294m. The domain length was 294m also. The model had an initial depth of 24m, filled with particles on an initially spacing of 0.5m. Contours of the pressure for 16m high waves are shown in Figure 2. Also shown in this figure are a few particle paths that display the combination of circular motion with the Stokes' drift in the direction of wave propagation. Although not shown, the velocity distribution within the wave correlates well with the theoretical distribution.

For a similar test case of regular, 4.0m high and 73.5m long waves the computed vertical velocity profile of a selected particle in the domain is compared to the analytical result in Figure 3. Even for this case with its higher wave steepness, there is an excellent agreement between simulated and analytical solutions.

From these results, the wave dynamics are concluded as correct within the domain of interest and hence are suitable for the study of the response of floating objects.

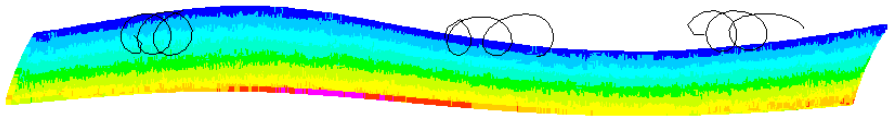

Figure 2: Pressure contour and selected particle trajectories for the 16m high 294m long wave

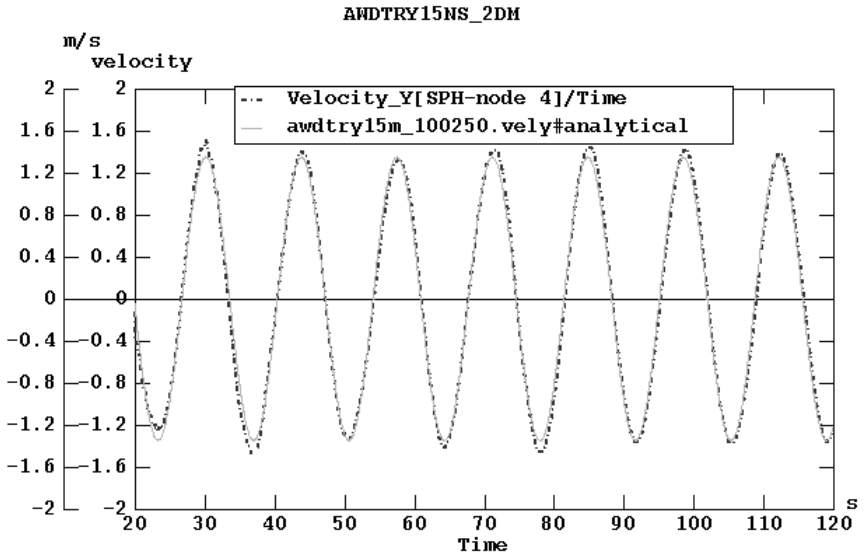


Figure 3: Time histories of the vertical velocity of a selected particle compared to the second-order analytical solution. For clarity the initialization phase is deleted in this figure

## 4 IMPACT OF A FLEXIBLE CYLINDER

To demonstrate that the coupled SPH-FE approach is able to simulate fluid-structure effects relevant for hydro-elasticity as may occur during ship slamming, the results from a simulation of an aluminium cylinder falling from 1m onto calm water are presented. Experimental results for this case and its numerical simulation including the effects of hydro-elasticity have been reported by Arai [12]. Numerical simulations by a coupled Euler-Lagrange approach, including the effects of water compressibility and entrapped air, have been reported by Bereznitski using MSC-DYTRAN, a coupled Euler-Lagrange code [13]. A comparison is made here between a fully FE solution and a combined FE and SPH solution. The combined solution employed SPH in the inner fluid region where

splash is anticipated, and FE elements in the regions further from the impact site. The tied contact between the SPH and FE elements noted in Section 2.2 maintains continuity throughout the domain. The simulation was done in 2D, did not include air and used elastic shell elements for the cylinder with a material modulus of 75GPa and a Poisson's ratio of 0.34. The 3mm thick aluminium cylinder had an outer diameter of 306mm.

Initial simulations revealed a relatively small nominal size of 4.1mm for the particles and finite elements was required in the impact region to maintain stability and capture transient events. It was also found that a first-order polynomial equation of state (EOS) for the water gave better results than the Murnaghan equation of state used in the previous examples. Using the actual compressibility of water, the polynomial EOS revealed propagation of compression waves following the impact. The same EOS material model has been used for particles and elements representing water. Artificial viscosity parameters for $\alpha$ and $\beta$ of 0.005 and 0.0 respectively were found to produce proper splashing. The fluid viscosity corresponding to these values is higher than that of water, but viscosity is believed to be a less important effect during slamming [14]. Simulation results showing the location of the cylinder and the outline of the free surface, as well as contours of the velocity magnitude in the upper part of the computational domain, for the mixed, as well as the pure FE computations, are shown in Figure 4. The equivalent stresses at the bottom element of the cylinder for the pure FE model and the combined SPH-FE model were found to be in good agreement with each other. For the cylinder deformation of Figure 5, the agreement in amplitude with that of Arai and that of Bereznitski is quite good, although the period of vibration is different. A suggested reason for this difference is possible sliding and separation of the water along the cylinder which is treated differently by the various numerical approaches [13].

It may be concluded from these results that the mixed SPH-FE enables the interaction between water and deformable, thin-walled structures to be modelled accurately, provided that the particle distribution is reasonably fine and that some parameter recommendations are adhered to. In this particular case, there is no specific preference for either model, but for cases with more complex (3D) geometry or more violent interaction, the finite element model will definitely break down due to element tangling, whereas SPH would have no problems continuing.

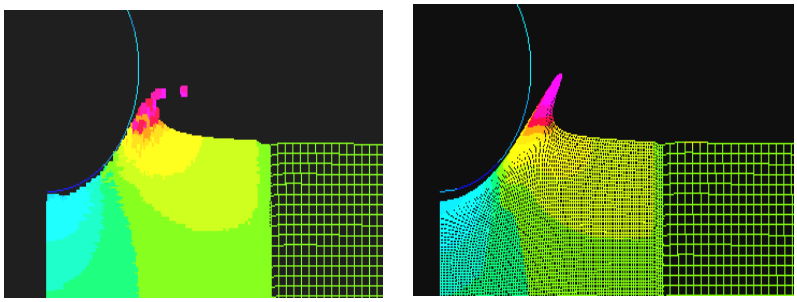

Figure 4: A segment of the FE (left) and SPH and FE (right) simulations in PAM-CRASH. Contours indicate velocity magnitudes, showing good correlation with each other.

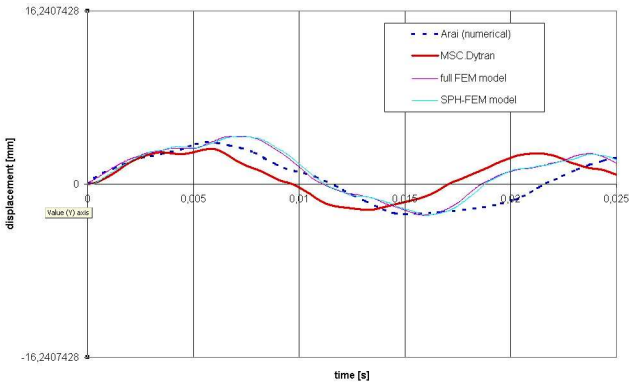


Figure 5: Time history of the deformation of the cylinder bottom for the FE simulation (purple) and SPH model (light blue) vs. the numerical results from Arai and Bereznitski (MSC-Dytran) for a drop height of 0.75 m.

## 5 GENERIC FRIGATE IN HIGH SEAS

This feasibility study focuses on the fluid-structure interaction (hydro-elasticity) related to the global deformation of the hull of a generic frigate subjected to high waves. Although the software is capable of utilising a fully deformable FE model of a frigate, such an FE model was not available to the authors. The model used here represents a greatly simplified tow-tank model technique used to acquire global loads with a segmented rigid body hull model [15], except that here the vessel is modelled at full scale.

The model developed is of a fast naval mono-hull of 147m LOA and approximately 5800 tonne displacement. The hull has been modelled by shell elements that are divided into 7 rigid-body segments along the length. These rigid body segments are connected to a deformable backbone structure modelled by 6 elastic shell elements. The flexible backbone begins at the centre of gravity of the foremost rigid body section and extends to the centre of gravity of the aftmost rigid body section. The backbone stiffness is of constant section and was deliberately chosen to be more flexible than that of a similarly sized "real" vessel. This greater flexibility enables the hog and sag bending to be observed more readily in the graphical output. The mass and moments of inertia of the model are believed to be reasonable for a vessel of this size. To investigate the effect of the backbone flexibility on the resulting forces experienced by the hull sections, two models have been developed, a 'flexible' model and a 'stiff' model with twice the stiffness of the 'flexible' model. More details of the numerical model and additional results may be found in Groenenboom et al. [16]. The simulation period began with the frigate above the mean water level, from where gravity acted on the vessel and the water to bring the vessel to a floating equilibrium position. A small amount of nodal damping was applied during the initial stages to suppress unrealistic responses from the settling process. The wave motion was developed over 20 seconds.

Two simulations have been conducted, one for each backbone stiffness. Both simulations have been performed over a simulation period of at least 60 seconds. Comparing the water level at the two gauges far in front and behind the ship for the flexible and stiff model reveals that the vessel flexibility has no discernable effect on the waves at remote locations. This is encouraging as there should be minimal effects of vessel flexibility on the wave profile at these distances away from the vessel.

Near the end of the simulation period, the flexible model shows large sag motions with some green water coming over the bow, as shown in Figure 6. Whilst this green water is not anticipated for the real vessel in 8m waves of this length, it must be appreciated that although this vessel has similar mass and inertias to a full size vessel, it has significantly less bending stiffness. Consequently it is expected that the hog and sag for this model will be greater than that of the real vessel, and hence the presence of green water on deck is likely.

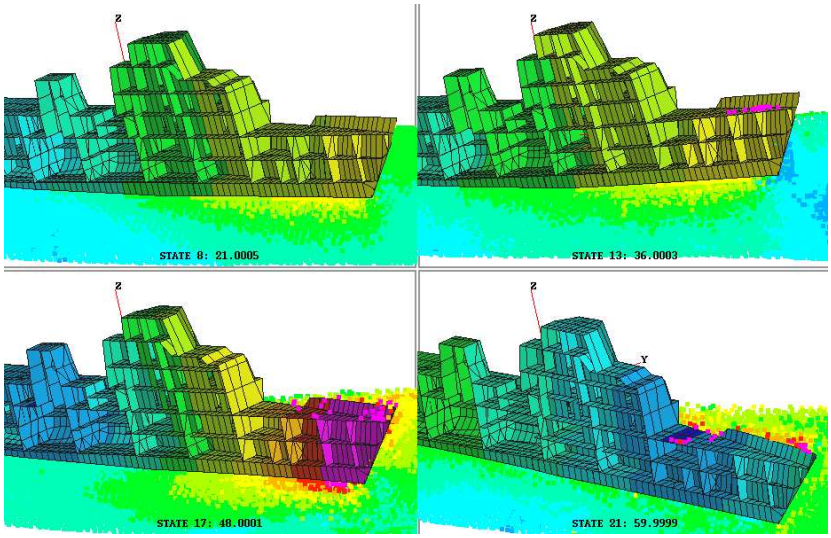


Figure 6: Contours of the velocity magnitude up to 4.1 m/s of the frigate and the water at 21, 36, 48 and 60 seconds.

Figure 7 compares the hydrodynamic forces with time on rigid body segments 1 (bow) and 5 (mid-ship) for the flexible and stiff vessels. It is observed that the stiff model experiences higher loads than the flexible model and that the bow segment of the stiff model is out of the water for a longer duration than for the flexible model. Conversely, the flexible model experiences lower forces, with the bow remaining submerged for longer, as would be expected intuitively.

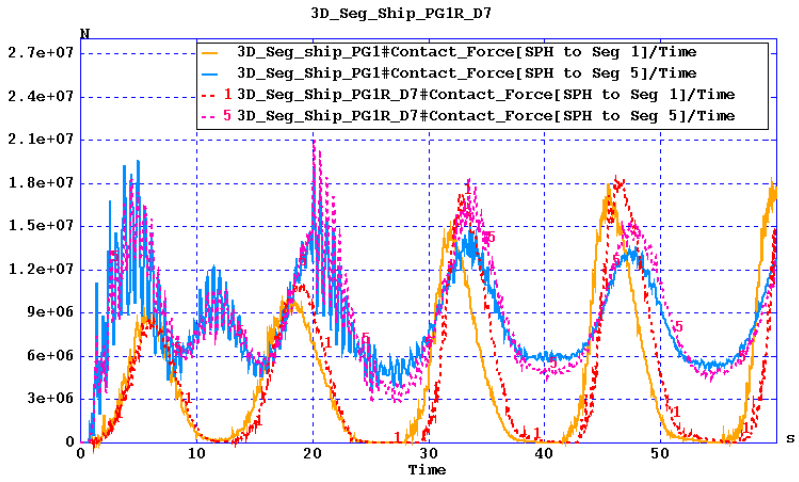


Figure 7: Time histories of the hydrodynamic forces on the first and the fifth segment for the stiff (PG1R) and the flexible model (PG1).

## 6 HELICOPTER DITCHING

Helicopters are an essential transport mechanism in many civilian and defence scenarios, often flying over water. In civilian scenarios, the helicopter is often acting as a ferry service for workers to offshore structures such as oil platforms. Even though in this situation the passengers and crew are trained in HUET (Helicopter Underwater Emergency Training), the survival rate is still alarmingly low for the (thankfully) low number of crashes or ditchings into the ocean. Statistics from helicopter accidents occurring into water [17] indicate that most fatalities occur from drowning, not injury attributable to the structural failure of the helicopter. Following drowning, the next most likely cause of death in accidents over water is by hypothermia. It is also noted from the number of accidents that in nearly 60% of the accidents, the helicopter inverted and sank "almost immediately". Such a response by the helicopter in water provides very little opportunity for egress of the crew and is a contributor to the high rate of drowning fatalities.

External Flotation Systems (EFS) for helicopters have been used operationally since the mid 1990's [18]. These provide a vast improvement in crew survivability of a helicopter ditching. The current situation is that EFS are seldom deployed. Even when required to do so, they do not always deploy as intended and consequently do not operate successfully when needed. Recent developments in the numerical simulation of airbag systems for automotive applications and the use of SPH technology for maritime studies has enabled a marriage of the two technologies to simulate the impact of a helicopter on a water surface, complete with the inflation of the EFS device. This provides a capability to simulate EFS systems for new helicopters, and the virtual try-out of new EFS systems that may be lighter and/or more effective than current designs. A generic implementation of the technology is shown in Figure 8. The simulation consists of a generic helicopter that is falling under gravity, a body of water, a tank for containment of the water, and the airbags fitted to the helicopter. The simulation is conducted at full size and in real time. The helicopter mass was 8800 kg.

The simulation of the helicopter without airbags displays the reported characteristics of initially floating whilst upright, subsequently rolling over, and finally sinking [19]. The loss of watertight integrity by the helicopter through doors and windows results in a rapid ingress of water, a loss of buoyancy and the sinking of the helicopter within 10 seconds of impact. The novel application of airbag simulation technology to provide the buoyancy is now described.

The helicopter EFS consists of four independent airbag chambers, each folded into a compact format for stowage during flight. In practice, inflation of the airbags is triggered just prior to, or on contact with, the water surface. The sliding interface noted in Section 2.2 acting between the flexible airbags and the particles ensures the particles remain on the outside of the airbag, thus providing flotation. A similar interface is defined between the SPH and the body of the helicopter. The doors are not part of this contact as typically the doors will be removed on impact to allow egress of the occupants. So obviously, the doors do not retain a watertight seal on immersion. Windows are typically not designed to be watertight to immersion. Hence, water ingress through the doors and windows is likely and handled in this simulation scenario.

Model configuration includes the initial folding of the airbag, such that it will unfold on inflation to the correct shape. An airbag folding algorithm is employed within the software [20]. This algorithm adjusts the geometry of the un-inflated flat airbag according to user-defined 'folds'. The result is a re-meshed finite element model of the airbag in a folded arrangement. It is important that the airbag does not tangle with the helicopter structure during inflation. Similarly, incorrectly inflated or punctured airbags will influence with the buoyancy provided to the helicopter. Thus, simulation of the inflation process allows an assessment of the design of the total EFS system.


Figure 8: Generic Helicopter with inflating flotation devices.

The airbag model used for the flotation devices is a large version of that used for automotive safety airbag simulation [3]. Membrane elements are available to model the anisotropic behaviour of common airbag materials, and to enable modelling of the wrinkling of the fabric-based materials. The membrane material has stiffness that results in a small increase in volume when the design pressure is achieved. Specific CFD algorithms have been developed for gas flow in the complex geometry of unfolding airbags, but in this case, the assumption that pressure and temperature are uniform in the bag may be assumed to be adequate. Permeability of the fabric material model may also be included to simulate the effect of loss of gas. The inflation of the flotation devices is controlled by a function that defines the flow rate of the gas. Figures 9a and 9b show the respective time histories of the pressure in the airbags and the volume of the airbags. Chamber 1 is an aft flotation device, and Chamber 4 is a forward flotation device. The x-axis is the time from the start of the simulation.

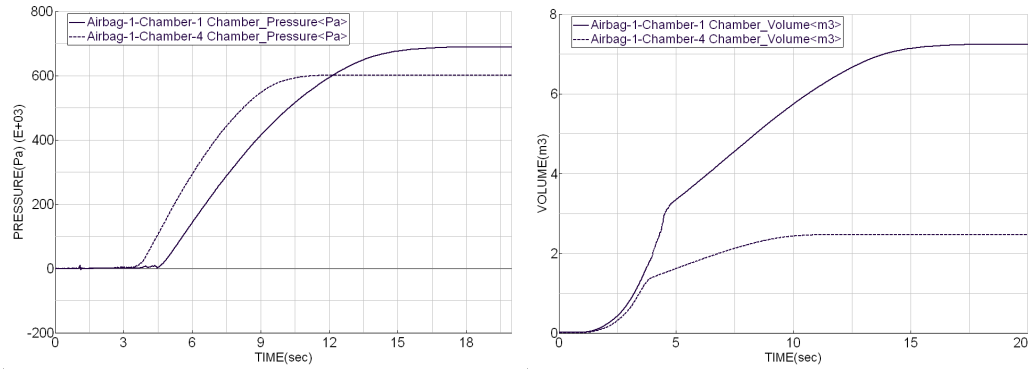


Figure 9.a and 9.b: Chamber pressure and Chamber volume for the rear and front EFS.

A few stages of the EFS unfolding is shown in Figure 10. Figure 8 shows the successful deployment of the EFS, resulting in a stable and upright floating helicopter from which occupant egress can be managed easily, thereby increasing occupant safety.

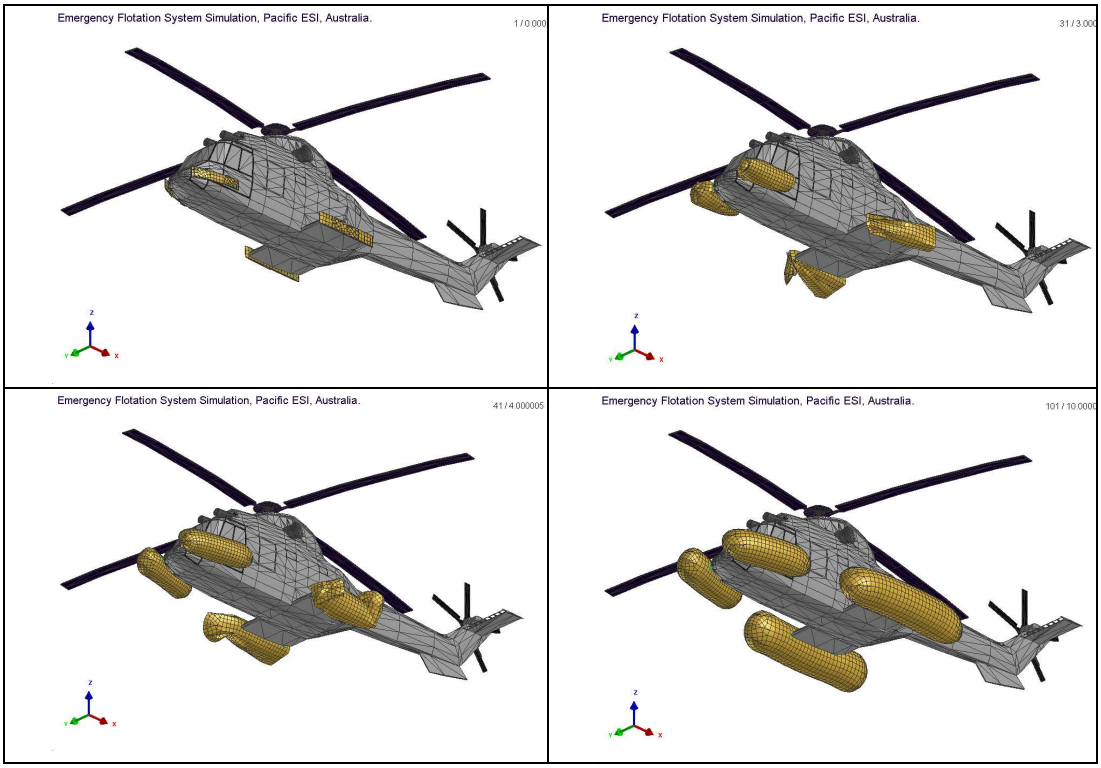


Figure 10: Inflation of the EFS on a helicopter.

## 7 DISABLED SUBMARINE

When a submarine loses all or some of its operational capability, it usually floats on the surface to undergo repairs or wait for assistance. The roll response of a surfaced submarine is notably worse than a naval ship of similar size, largely due to the low righting moment in roll and the circular hull sections required for the pressure-hull. Consequently there is high likelihood of crew illness due to excessive roll motions of the disabled submarine wallowing on the surface.

A submarine with 6 degrees of freedom and zero forward speed was placed at 45 degrees to a single frequency wave system to observe the response of the vessel. The submarine was 110m long, with an external hull of 9.75m diameter, and a nominal displacement of 6100 tonne. The submarine was modeled as a rigid body of shell elements. The location of the centre of gravity was found by trial and error until the vessel floated with a level trim in calm water.

The wave was modeled with SPH using the moving-floor technique discussed in Section 3, and hence, no paddles were required to generate the wave. The wavelength was 147m and wave height 2.5m. Periodic boundary conditions were placed at the one wavelength limit. The nominal depth was 15m, obtained using 128,000 SPH elements

in an initially close-packed hexagonal arrangement. The top view of the model setup is shown in Figure 11.

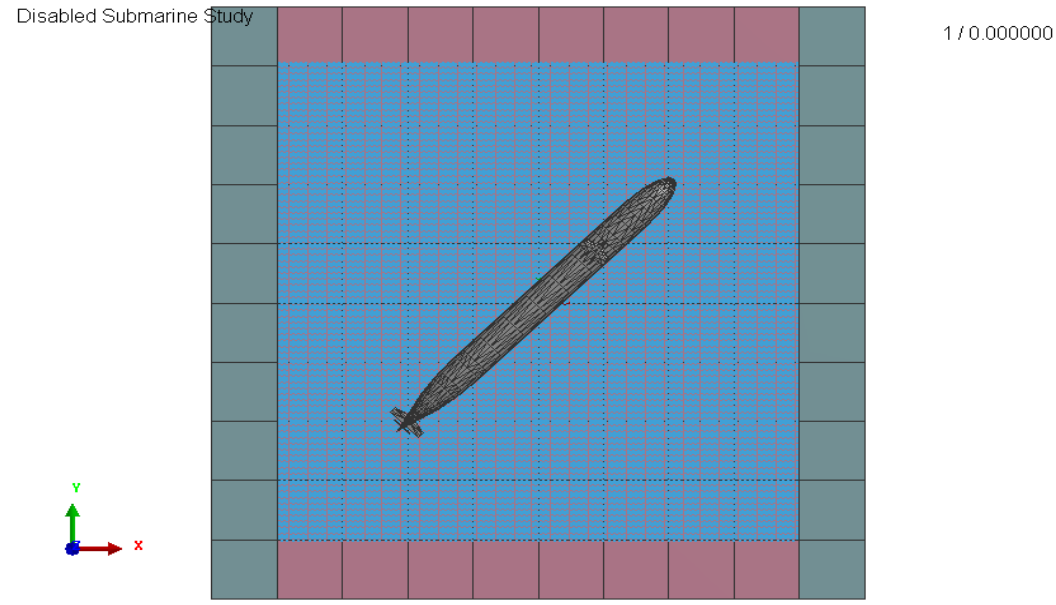


Figure 11: General arrangement of the submarine oblique to the waves. The waves travel from right to left. The squares elements are the floor segments.

Figure 12 shows the submarine after 300 seconds of simulation. The colour gradient is the coordinate of the surface SPH elements graded to give the impression of a wave with dark colour being the trough and the lighter shade the wave crest.

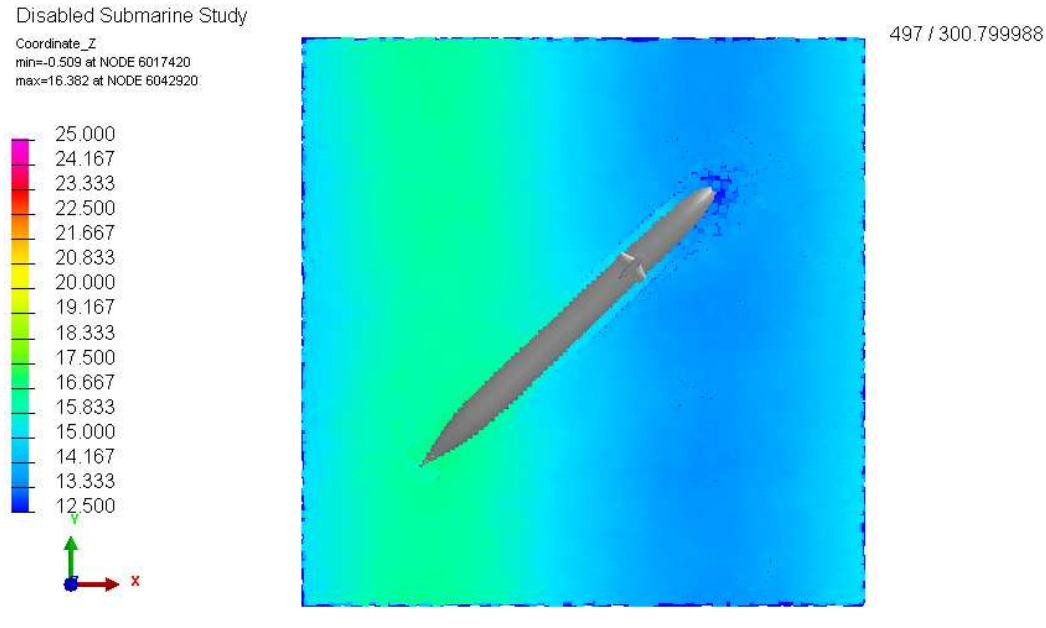


Figure 12: Top view of the submarine after 300 seconds of simulation.

The submarine displays a corkscrewing motion, typical of a roll-pitch coupled response of a vessel. The vessel drifts with the waves slowly as shown in the coordinate of the CG with time shown in Figure 13. The first 50 seconds of the simulation is required to achieve a dynamic equilibrium in the wave train. The progressive yaw rotation from the initial position is shown as the Z axis rotation in Figure 14. This shows a steady turning of the vessel into the waves.

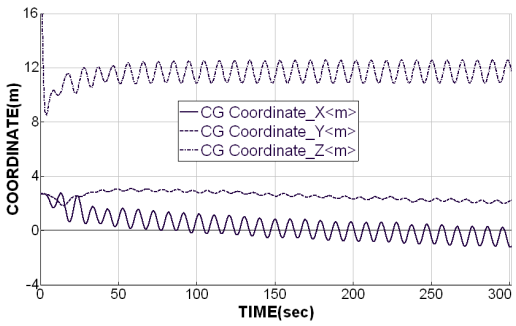


Figure 13: Coordinate of the CG of the submarine with time, showing the gradual drift in the X and Y directions.

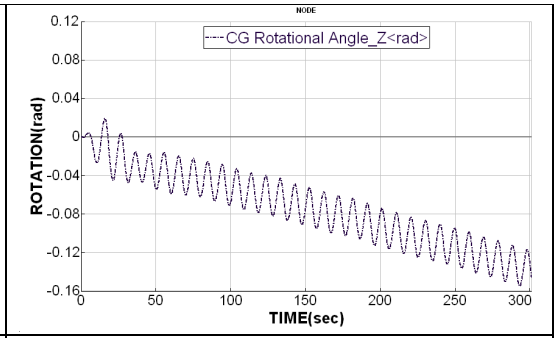


Figure 14: Yaw of the submarine is increasing with time indicating a bow-to-the wave position is being adopted.

Of these results, it is Figure 14 that is most revealing in terms of designing passive devices that may improve the roll motions of the submarine. Beam-on seas would typically result in the most severe roll motions for a vessel in a seaway, and bow-on would produce the most comfortable roll motions. Hence, the passive reduction of the yaw angle shown in Figure 14 suggests the shape of this submarine is working to reduce the yaw angle of the vessel. For more dramatic effects on yawing the vessel into the waves, and thus reducing roll motions of the submarine, simulations of deployable features could be simulated with the aim of making the vessel more comfortable for the crew until assistance has arrived.

## 8 CONCLUSIONS

The coupled FE-SPH approach has been shown to be capable of simulating fluid-structure interaction in a variety of dynamic maritime phenomena. Cross-industry exploitation of mature software tools, such as those used to investigate airbag behaviour, and even the SPH, method itself brings mature simulation capability to new industry sectors. The real-world applications are limited only by our imagination and to some extent, the computing power at our disposal.

## 9 ACKNOWLEDGEMENTS

The authors would like to acknowledge the work of our colleague Allen Chhor in developing the helicopter ditching simulations with inflating airbags, and Damian McGuckin for reviewing this paper. This work forms part of a multi-year, internal R+D project within Pacific Engineering Systems International.

## REFERENCES

[1] B. Cartwright, J. Xia, S. Cannon, D. McGuckin, P. Groenenboom, Motion Prediction of Ships and Yachts by Smoothed Particle Hydrodynamics, *2nd High Performance Yacht Design Conference,* Auckland, NZ (2006).

[2] P. Groenenboom and B. Cartwright, "Hydrodynamics and fluid-structure interaction by coupled SPH-FE method", *Journal of Hydraulic Research* Vol. **47**, Special Issue (2009), pp. 1–13 (2009).

[3] PAM-CRASH Theory Notes Manual, ESI-Group, 2009.

[4] MONAGHAN, J.J., 'Simulating free surface flows with SPH', *J. Comp. Phys.*, **110**, (1994).

[5] MONAGHAN, J.J., 'Smoothed Particle Hydrodynamics', *Annual Review of Astronomy and Astrophysics, 30, pp 543–574,* 1992.

[6] M. Meywerk, F. Decker and J. Cordes, "Fluid-structure interaction in crash simulation", *Proc. Inst. Mech. Engrs*., **214**, 669-673 (1999).

[7] C. Haack, On the use of a Particle Method for Analysis of Fluid-structure Interaction. *Sulzer Innotech Report STR_TB2000_014*, June (2000)

[8] H. Climent, L. Benitez, F. Rosich, F. Rueda and N. Pentecote, Aircraft Ditching Numerical Simulation, *25th International Congress of the Aeronautical Sciences,* Hamburg, Germany (2006).

[9] P. Groenenboom, Lifeboat water entry simulation by the hybrid SPH-FE method, *IIIrd ERCOFTAC SPHERIC WORKSHOP , EPFL, Ecole Polytechnique Fédérale de Lausanne, Switzerland* (2008)

[10] B. Cartwright, P. Groenenboom and D. McGuckin, A Novel Technique to Predict Non-Steady Loads in Vessels in Severe Seas. *ISOPE* , Toulon, France (2004).

[11] B. Cartwright, D. McGuckin, T. Turner and S. Cannon., "The Modelling of Landing Craft Motions inside a flooded Well dock using Smoothed Particle Hydrodynamics", *PACIFIC* Sydney, Australia, (2006).

[12] M. Arai and T. Miyauchi , "Numerical study of the impact of water on cylindrical shell, considering fluid-structure interaction", *PRADS* Conference (1998).

[13] A. Bereznitski, "Local hydroelastic response of ship structures under impact loads from water", *PhD thesis*, Delft University of Technology, The Netherlands (2003).

[14] O. Faltinson, Challenges in experimental and numerical modelling with emphasis on high-speed marine vehicles and sloshing, *ICMRT '07*, Ischia, Italy, (2007).

[15] K. McTaggart, I. Datta, S. Stirling, S. Gibson and I. Glen, Motions and Loads of Hydroelastic Frigate Model in Severe Seas, *Report Number 504187*, Defence Research and Development Canada (1997).

[16] P. Groenenboom., B. Cartwright and D. McGuckin, Numerical Simulation of Ships in High Seas using a Coupled SPH-FE Approach, *RINA Int'l Conference on Innovation in High Speed Marine Vessels*, Fremantle, Australia (2009).

[17] CAA PAPER 2005/06, Summary Report on Helicopter Ditching and Crashworthiness Research, Civil Aviation Authority, Safety Regulation Group, 2005.

[18] M. Hamer, Air bags for choppers, New Scientist **2094** (09 August 1997)

[19] B. Cartwright, Ditching Behaviour and Sinking of Helicopters, *International K-Rash Users Symposium*, Stuttgart, 2009.

[20] "Visual Safe" Graphical User Interface, ESI-Group, 2009.